

Analytic and Algorithmic Solution of Random Satisfiability Problems

M. Mézard,¹ G. Parisi,^{1,2} R. Zecchina^{1,3*}

We study the satisfiability of random Boolean expressions built from many clauses with K variables per clause (K-satisfiability). Expressions with a ratio α of clauses to variables less than a threshold α_c are almost always satisfiable, whereas those with a ratio above this threshold are almost always unsatisfiable. We show the existence of an intermediate phase below α_c , where the proliferation of metastable states is responsible for the onset of complexity in search algorithms. We introduce a class of optimization algorithms that can deal with these metastable states; one such algorithm has been tested successfully on the largest existing benchmark of K-satisfiability.

The K-satisfiability problem (Ksat) asks whether one can satisfy simultaneously a set of M constraints between N Boolean variables, where each constraint is a clause built as the logical OR involving K variables (or their negations). Ksat is at the core of combinatorial optimization theory (1) and often serves as a benchmark for search algorithms in artificial intelligence and computer science. An efficient algorithm for solving Ksat for $K \geq 3$ would immediately lead to other algorithms for efficiently solving thousands of different hard combinatorial problems. The class of combinatorial problems sharing such a crucial feature is called NP-complete (2), and it is a basic conjecture of modern computer science that no such efficient algorithm exists. Algorithms that are used to solve real-world NP-complete problems display a huge variability of running times, ranging from linear to exponential. A theory for the typical-case behavior of algorithms, on classes of random instances chosen from a given probability distribution, is therefore the natural complement to the worst-case analysis (3–5). Whereas 1sat and 2sat problems are solved efficiently by polynomial time algorithms (6), $K > 2$ randomly generated Boolean formulae may become extraordinarily difficult to solve: It has been observed numerically (7, 8) that computationally hard random instances are generated when the problems are critically constrained [i.e., close to the satisfiable-unsatisfiable (SAT-UNSAT) phase boundary]. The study of critical instances represents a theoretical chal-

lenge toward a greater understanding of the onset of computational complexity and the analysis of algorithms. Moreover, such hard instances are a popular test bed for the performance of search algorithms (9).

The random Ksat problem has close similarities with models of complex materials such as spin glasses, which are fundamental systems in the statistical physics of disordered systems (10). Spin glasses deal with binary variables (“spins”) interacting with random exchange couplings. Each pair of interacting spins can be seen as a constraint, and finding the state of minimal energy in a spin glass amounts to minimizing the number of violated constraints. Although the constraints in spin glasses and Ksat differ with respect to their precise form, in both cases the difficulty comes from the possible existence of “frustration” (11), which makes it difficult to find the global optimal state by a purely local optimization procedure. Links between combinatorial optimization and statistical physics have been known for years (10, 12, 13). Techniques from statistical physics are particularly useful when the size of the instance is large.

Two main categories of questions can be addressed. One type is algorithmic (e.g., finding an algorithm that decides whether an instance is SAT or UNSAT, or that tries to minimize the number of violated constraints). Another one is more theoretical and deals with random instances for which one wants to predict the typical behavior (e.g., phase transitions and structure of the solution space).

We address the two types of questions in the 3sat problem. When the numbers of variables N and of clauses M both increase at a fixed value of $\alpha = M/N$, random Ksat problems become generically SAT at small α and generically UNSAT at large α . The existence of a SAT-UNSAT phase transition in the infinite N limit has been established rigorously for any K (14), but the critical value α_c

(that separates the two phases) has been found only in the (polynomial) $K = 2$ problem where $\alpha_c = 1$ (15–17). For the NP-complete case $K \geq 3$, much less is known. The present best numerical estimate for α_c at $K = 3$ is 4.26 (18), and the rigorous bounds are $3.42 < \alpha_c < 4.506$ (19, 20); previous statistical mechanics analysis, using the replica method, has found $\alpha_c(3) \sim 4.48$ (21) and $\alpha_c(3) \sim 4.396$ (22) in the framework of variational approximations. The SAT-UNSAT decision problem is also known experimentally to be algorithmically harder to solve in the neighborhood of α_c , depending on the characteristics of the SAT-UNSAT phase transition. Indeed, 2sat and 3sat are different in this respect (23).

Setting out the statistical physics problem. The Ksat problem deals with N Boolean variables x_i , $i \in \{1, \dots, N\}$. Each clause $a \in \{1, \dots, M\}$ involves K variables $\{x_{i_1(a)}, \dots, x_{i_K(a)}\}$. Each such variable can be negated or not, and the clause is built as the OR function of the K resulting variables. In physical terms, the variable x_i can be represented by a “spin” $s_i = \pm 1$ through the one-to-one mapping $s_i = -1$ if x_i is false and $s_i = +1$ if x_i is true. For each variable $x_{i_k(a)}$ appearing in clause a , one introduces a “coupling” $J_a^k = -1$ if the variable appears negated in the clause; otherwise the coupling is $J_a^k = 1$. The sets of indices $i_1(a), \dots, i_K(a)$ and of “couplings” $\mathbf{J}_a = \{J_a^1, \dots, J_a^K\}$ define an instance of the problem under study. Given a spin configuration, the “energy” $\epsilon_{\mathbf{J}_a}(s_{i_1(a)}, \dots, s_{i_K(a)})$ of clause a is equal to 0 if the clause is satisfied, or equal to 1 if it is violated (24). The total energy E equals the number of violated clauses.

In statistical physics, one assigns to each of the 2^N spin configurations a Boltzmann probability $\exp(-\beta E)/Z$, where β is an auxiliary parameter playing the role of the inverse of temperature, and Z is a normalization term; here we are interested in the $\beta \rightarrow \infty$ “zero-temperature” limit, where Boltzmann’s law selects optimal states.

The spin glass approach. We first study the large N limit of the random 3sat problem, where the indices in each clause are chosen randomly, as well as the sign of each coupling, with uniform distributions. Our approach to these problems uses a general strategy initiated years ago in spin glass theory (10). The first concept we need to introduce is that of a state. Roughly speaking, states correspond to connected regions of configurations, such that one must cross energy barriers that diverge when $N \rightarrow \infty$ to go from one state to another. The archetype of such a situation is the ferromagnetic transition where the spins collectively polarize, either toward an “up” state or toward a “down” state. In frustrated systems such as satisfiability problems, many states can exist: The

¹Laboratoire de Physique Théorique et Modèles Statistiques, CNRS and Université Paris Sud, Bât. 100, 91405 Orsay Cedex, France. ²Sezione INFN, SMC and UdRm1 of INFN, Università “La Sapienza,” P.le A. Moro 2, 00185 Roma, Italy. ³Abdus Salam International Centre for Theoretical Physics, Str. Costiera 11, 34100 Trieste, Italy.

*To whom correspondence should be addressed. E-mail: zecchina@ictp.trieste.it

number of states with energy E behaves as $\exp[N \Sigma(e)]$, where $e \equiv E/N$; the function $\Sigma(e)$, called the complexity, is a crucial concept in studies of structural glasses. The ground-state energy density e can be found by the condition $\Sigma(e) = 0$. Here we choose a restricted zero-temperature definition that applies to random Ksat: A state is simply a cluster of configurations of equal energy related by single spin-flip moves, such that the energy cannot be decreased by any sequence of single spin flips (25). Generalizing the approach of (26), one can develop a whole “zero-temperature thermodynamics” of the states by introducing a “free energy” function $\Phi(y)$ defined from

$$\exp[-Ny\Phi(y)] = \int de \exp[N[\Sigma(e) - ye]] \quad (1)$$

The reweighting y is a Lagrange parameter (similar to an inverse temperature) that allows the energy of the states to be fixed. Larger reweighting selects states of lower energies until one reaches $y = y^*$, corresponding to the lowest energy states ($y^* = \infty$ in the SAT region).

The cavity method: Message-passing procedures. To compute $\Phi(y)$, we use the zero-temperature cavity method (27, 28), in which the basic ingredients are the cavity fields and the cavity biases, which are defined in each state. The cavity field $h_{i \rightarrow a}$ measures the tendency of spin i to be up, when one of the clauses, a , to which i belongs, has been disconnected (Fig. 1). It is equal to the sum of cavity biases $u_{b \rightarrow i}$, sent to site i from all the other clauses b to which it belongs. In computer science terminology, cavity fields are messages sent from a variable node to a function node, whereas cavity biases are messages sent from a function node to a variable node (29). The cavity biases are determined by a local optimization procedure. Consider one clause a , involving K variables s_1, \dots, s_K , and a penalty function $\epsilon_j(s_1, \dots, s_K)$. The optimization on the variables s_2, \dots, s_K , expressed as

$$\begin{aligned} \min_{s_2, \dots, s_K} & \left(\epsilon_j(s_1, \dots, s_K) - \frac{1}{2} \sum_{j=2}^K h_j s_j \right) \\ & = -\frac{1}{2} [a_j(h_2, \dots, h_K) + s_1 u_j(h_2, \dots, h_K)] \end{aligned} \quad (2)$$

defines the mean energy shift a_j and the cavity bias $u_{a \rightarrow 1} = u_j(h_2, \dots, h_K)$ propagated from this clause to the variable s_1 (30).

The advantage of cavity biases and cavity fields in large ($N \gg 1$) random Ksat and spin glass problems is the special structure of the interaction graph: It is locally tree-like, and the connectivity fluctuates from site to site with a Poisson distribution of mean $K\alpha$ (see Fig. 1). On a more global scale, these random

graphs have loops with a typical length growing as $\log(N)$. As the cavity fields h_2, \dots, h_K are defined in the absence of the clause, they correspond to faraway variables [with a distance of order $\log(N)$]. The “clustering property,” valid inside each state, implies that their correlations go to zero at large N (on a real tree they would be fully uncorrelated). The topology of the graph implies that the cavity equations are exact on finite subgraphs.

To determine the statistical properties of the set of cavity biases and how they change from state to state, we introduce “surveys,” which are histograms of cavity biases. For each state ω , there is one cavity bias $u_{a \rightarrow 1}^\omega$ propagated from one clause a to site 1; it can be computed from Eq. 2, where the cavity fields are those corresponding to the state ω . For a given value of the reweighting, the survey propagated to spin s_1 in Fig. 1 is defined as $Q_{a \rightarrow 1}^{(y)}(u) = C \sum_\omega \delta(u - u_{a \rightarrow 1}^\omega)$, where C is a normalization constant ensuring that $Q_{a \rightarrow 1}^{(y)}(u)$ is a probability distribution, and the sum over ω is restricted to the states having the energy density e selected by the reweighting y .

The survey propagation rules on the graph of Fig. 1 take the precise form

$$\begin{aligned} Q_{a \rightarrow 1}^{(y)}(u) &= C' \int \prod_{r=1}^q dw_r Q_{b_r \rightarrow 2}^{(y)}(w_r) \\ & \int \prod_{s=1}^{q'} dv_s Q_{c_s \rightarrow 3}^{(y)}(v_s) \\ & \delta[u - u_j(W, V)] \exp[y a_j(W, V)] \end{aligned} \quad (3)$$

where $W = w_1 + \dots + w_q$, $V = v_1 + \dots + v_{q'}$, and C' is a normalization constant. The exponential term in Eq. 3 takes care of the energy-level crossings induced by the propagation. Once the surveys are known, the free energy $\Phi(y)$ can be computed using the formulae of (27, 28), and the complexity can be deduced from Eq. 1. The order parameter of the theory is the collection of the surveys.

Phase diagram. In the zero-temperature 3sat problem, one sees from the definition (2) that a given cavity bias $u_{a \rightarrow i}$ takes either the values $\{0, 1\}$ (if the variable x_i appears negated in clause a) or the values $\{0, -1\}$. The corresponding survey $Q_{a \rightarrow i}^{(y)}(u)$ is thus characterized by a single number, the probability that $u = 0$. Using this simplification, we have been able to compute (31) the statistical distribution of surveys in random graphs in the infinite volume limit. We find two critical

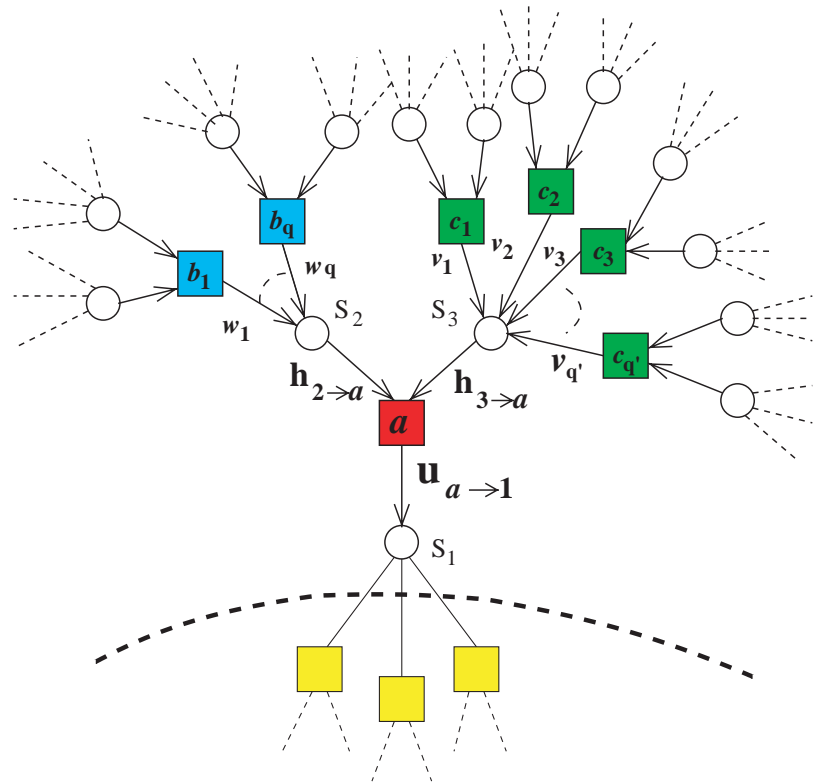


Fig. 1. In the random 3sat problem, the graph of clauses is locally isomorphic to a tree. Variables (spins) are depicted by a circle, and clauses by a square. The cavity bias $u_{a \rightarrow 1}$ sent from the red clause a to the variable s_1 summarizes the effects of optimizing clause a on s_2, s_3 , taking into account all the blue + green (top) part of the graph, when the yellow (bottom) part has been taken away. In the absence of the red clause, the cavity field $h_{2 \rightarrow a}$ sums up all cavity biases w_1, \dots, w_q arriving onto s_2 from the blue clauses, and the cavity field $h_{3 \rightarrow a}$ sums up all cavity biases $v_1, \dots, v_{q'}$ arriving onto s_3 from the green clauses.

values of α at $\alpha_d \sim 3.921$ and $\alpha_c \sim 4.256$. For $\alpha < \alpha_d$, the solution is of a paramagnetic type [all the surveys equal $\delta(u)$], a generic instance is satisfiable, and the solution can be found even by a simple zero-temperature Metropolis algorithm (ZTMA) (32). For $\alpha_d < \alpha < \alpha_c$, the space of configurations breaks up into many states, and there exists a nontrivial complexity (33). Some of the states have zero energy; therefore, we are still in the SAT phase. It can be argued that algorithms like ZTMA will generically get trapped into the most numerous states, which have an extensive (proportional to N) energy E_{th} .

At $\alpha = 4.2$ we find analytically $E_{th} \sim 0.0036N$, and we have checked that ZTMA converges to a similar value of energy. The fact that $e_{th} = E_{th}/N$ is small explains the good performance of smarter algorithms on instances involving a few thousand variables. At $\alpha > \alpha_c$, the system is in its UNSAT phase, and the lowest possible energy is positive. The phase diagram is summarized in Fig. 2.

Survey propagation algorithm. We now consider one given instance (31), that is, one fixed large graph. We have seen experimentally that in the glassy region $\alpha > \alpha_d$, the standard ($y = 0$) iteration of cavity biases either ceases to converge or converges to the trivial paramagnetic solution where all $u_{a \rightarrow i} = 0$. If i is the r th site connected to the function node a , we introduce a survey $Q_{a \rightarrow i}^{(y)}(u) = \eta_{a \rightarrow i} \delta(u) + (1 - \eta_{a \rightarrow i}) \delta(u + J_a^r)$ that is characterized by the single number $\eta_{a \rightarrow i}$. The survey propagation of Eq. 3 performed with random sequential updating is a message-passing procedure that defines a dynamical process in the space of the KN variables $\eta_{a \rightarrow i}$. We have implemented it on large random instances in the hard part of the SAT phase, with $\alpha \sim 4.2$ to 4.25, using a sufficiently large value of y (typically $y \sim 4$ to 6). The process is found to converge to a unique nontrivial solution. We expect that this survey propagation technique can be of interest in many problems of statistical inference.

The set of all surveys $Q_{a \rightarrow i}^{(y)}(u)$ found after

convergence provides a nontrivial information on the structure of the states. From all the surveys sent onto one site i , we reconstruct through a reweighted convolution (34) the probability distribution of local fields on this site, $P_i(H)$. This is a distribution on integers $[P_i(H) = \sum_r \delta(H - r)w_i^r]$. The total weight $w_i^+ = \sum_{r=1}^{\infty} w_i^r$ of $P_i(H)$ on positive integers gives the fraction of zero-energy states where $s_i = 1$; similarly, the total weight $w_i^- = \sum_{r=-\infty}^{-1} w_i^r$ of $P_i(H)$ on negative integers gives the fraction of zero-energy states where $s_i = -1$. We have checked numerically, on single instances with $N = 10,000$, that these fractions predicted from survey propagation agree with those obtained by averaging on a few hundreds of ground states.

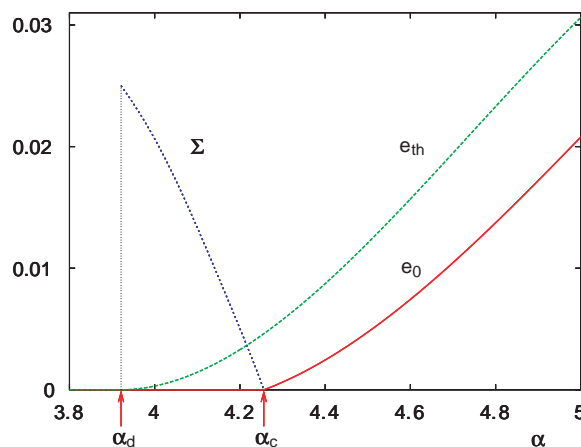
A decimation algorithm. This information can be exploited to invent new types of algorithms (31) or to improve existing ones. We have worked out one such application, the survey inspired decimation (SID), which shows promising performance, but other algorithms probably could be found using the same type of information. Given an instance, we first compute all the surveys by the survey propagation algorithm with a sufficiently large value of y (e.g., $y = 6$). Then we deduce the distribution of local fields, and in particular their weights w_i^\pm on positive and negative integers. We then fix the variable i with largest $|w_i^+ - w_i^-|$ to the value $s_i = \text{Sign}(w_i^+ - w_i^-)$. Satisfied clauses are eliminated, and unsatisfied K -clauses involving i are transformed into $K - 1$ clauses, leading to a new instance with a reduced number of variables (and of clauses). The surveys can be propagated again on this new instance (starting from the previous ones) until convergence, and the procedure is iterated. Whenever a paramagnetic state is found (signaled by all $\eta_{a \rightarrow i} = 1$) or at some intermediate steps, a rapid search process like simulated annealing at a fixed cooling rate is run.

This SID algorithm has been tested successfully on the largest (up to $N = 2000$) existing benchmarks (9) of random 3sat

instances in the hard regime. Satisfying assignments have been found for all benchmarks. We have applied the SID to much larger instances, increasing N up to $N = 10^5$ at a fixed $\alpha = 4.2$. The algorithm is very efficient: It always finds a SAT configuration, and its apparent complexity scales like N^2 , although more systematic studies with higher statistics will be necessary to establish this behavior. For the very same large instances, the only existing algorithm able to find solutions, at a considerable computational cost, is a highly optimized version of the walksat algorithm (9, 35).

Conclusions. We have proposed an analytical method that predicts quantitatively the phase diagram of the random 3sat problem in the limit of infinite number of clauses and opens the way to other types of algorithms. The existence of an intermediate phase with many metastable states close to the SAT-UNSAT transition explains the slowing down of algorithms in this region. We would like to stress that the solution we propose is typical of a “one-step replica symmetry-breaking” solution, as it is called in spin glasses (10). All the consistency checks of the analytic results lead us to believe that this solution is exact for the 3sat problem. From the strict mathematical point of view, the phase diagram we propose should be considered as a conjecture, as for the great majority of the theoretical results in statistical physics. Our computation implies that a way to provide a fully rigorous proof of the transition behavior in random Ksat problems could be based on the study of the decomposition of the probability measure into states endowed with the clustering property (36). On the other hand, the predictions of our theory can be compared with numerical experiments, and our first such tests have confirmed its validity. On the basis of the analytical study, our algorithm looks promising in that it can solve large instances exploring a rather small number of spin configurations. It will be interesting to explore its application to other optimization problems.

Fig. 2. The phase diagram of the random 3sat problem. Plotted is e_0 , the number of violated clauses per variable (red), versus the control parameter α , which is the number of clauses per variable. The SAT-UNSAT transition occurs at $\alpha = \alpha_c \sim 4.256$. The green line is e_{th} , the threshold energy per variable, where local algorithms get trapped. The blue line is the complexity Σ of satisfiable states, equal to $1/N$ times the logarithm of their number.



References and Notes

1. S. Cook, in *Proceedings of the 3rd Annual ACM Symposium on Theory of Computing* (Association for Computing Machinery, New York, 1971), p. 151.
2. M. R. Garey, D. S. Johnson, *Computers and Intractability: A Guide to the Theory of NP-Completeness* (Freeman, New York, 1979).
3. L. A. Levin, *SIAM J. Comput.* **14**, 285 (1986).
4. S. Ben-David, B. Chor, O. Goldreich, M. Luby, *J. Comput. Syst. Sci.* **44**, 193 (1992).
5. Y. Gurevich, *J. Comput. Syst. Sci.* **42**, 246 (1991).
6. B. Aspvall, M. F. Plass, R. E. Tarjan, *Process. Lett.* **8**, 121 (1979).
7. T. Hogg, B. A. Huberman, C. Williams, Eds., special issue on *Frontiers in Problem Solving: Phase Transition and Complexity*, *Artif. Intell.* **81** (1996).
8. O. Dubois, R. Monasson, B. Selman, R. Zecchina, Eds., special issue on *Phase Transitions in Combinatorial Problems*, *Theoret. Comp. Sci.* **265** (2001).
9. Satisfiability Library (www.satlib.org).
10. M. Mézard, G. Parisi, M. A. Virasoro, *Spin Glass Theory and Beyond* (World Scientific, Singapore, 1987).

11. A subset of variables is frustrated when it is impossible to assign these variables in such a way that the constraints are satisfied [see (10)].
12. Y. Fu, P. W. Anderson, *J. Phys. A* **19**, 1605 (1986).
13. O. C. Martin, R. Monasson, R. Zecchina, *Theor. Comp. Sci.* **256**, 3 (2001).
14. E. Friedgut, *J. Am. Math. Soc.* **12**, 1017 (1999).
15. A. Goerdt, in *Proceedings of the 17th International Symposium on Mathematical Foundations of Computer Science*, I. M. Havel, V. Koubek, Eds. (Springer-Verlag, Heidelberg, 1992), pp. 264–274.
16. V. Chvátal, B. Reed, in *Proceedings of the 33rd IEEE Symposium on Foundations of Computer Science* (IEEE Computer Society Press, Los Alamitos, CA, 1992), p. 620.
17. B. Bollobás, C. Borgs, J. T. Chayes, J. Han Kim, D. B. Wilson, *Rand. Struct. Alg.* **18**, 301 (2001).
18. J. A. Crawford, L. D. Auton, *Artif. Intell.* **81**, 31 (1996).
19. A. Kaporis, L. Kirousis, E. Lalas, in *Proceedings of the 10th European Symposium on Algorithms (ESA 2002)* (Springer-Verlag, Heidelberg, in press).
20. O. Dubois, Y. Boufkhad, J. Mandler, in *Proceedings of the 11th ACM-SIAM Symposium on Discrete Algorithms* (San Francisco, January 2000), pp. 124–126.
21. G. Biroli, R. Monasson, M. Weigt, *Eur. Phys. J. B* **14**, 551 (2000).
22. S. Franz, M. Leone, F. Ricci-Tersenghi, R. Zecchina, *Phys. Rev. Lett.* **87**, 127209 (2001).
23. R. Monasson, R. Zecchina, S. Kirkpatrick, B. Selman, L. Troyansky, *Nature* **400**, 133 (1999).
24. The energy of a clause can be written explicitly as $\epsilon_{j_a}(s_{j_1(a)}, \dots, s_{j_l(a)}) = 2^{-K} \prod_{i=1}^K (1 + J_i^a s_{j_i(a)})$.
25. In Ksat, it turns out that each state involves an exponentially large (in N) number of configurations.
26. R. Monasson, *Phys. Rev. Lett.* **75**, 2847 (1995).
27. M. Mézard, G. Parisi, *Eur. Phys. J. B* **20**, 217 (2001).
28. ———, <http://arxiv.org/abs/cond-mat/0207121> (2002).
29. F. R. Kschischang, B. J. Frey, H.-A. Loeliger, *IEEE Trans. Inf. Theory* **47**, 498 (2002).
30. For $K = 3$ one has $a_j(h_2, h_3) = |h_2| + |h_3| - \theta(J_2 h_2)\theta(J_3 h_3)$ and $u_j(h_2, \dots, h_K) = -J_1 \theta(J_2 h_2)\theta(J_3 h_3)$, with $\theta(x) = 1$ if $x > 0$ and $\theta(x) = 0$ if $x \leq 0$.
31. M. Mézard, R. Zecchina, <http://arxiv.org/abs/cond-mat/0207194> (2002).
32. In the ZTMA, one starts from a given configuration of energy E , picks up randomly one variable, and computes the new energy E' if this variable is flipped. The move is accepted (i.e., the variable is flipped) whenever $E' \leq E$; otherwise, the move is rejected. The procedure is then iterated.
33. This situation is familiar in mean field models of glasses, where α_d corresponds to a density of dynamical arrest, and α_c is the true transition point. For a review, see (37).
34. The explicit form is $P_i(H) = \int \prod_a [du_a Q_{a \rightarrow \cdot}(u_a)] \delta(H - \sum_a u_a) \exp(\gamma \sum_a u_a)$, where the index a spans all the function nodes connected to the variable i .
35. B. Selman, H. Kautz, B. Cohen, in *Proceedings of the Second DIMACS Challenge on Cliques, Coloring and Satisfiability*, M. Trick, D. S. Johnson, Eds. (American Mathematical Society, Providence, RI, 1993), p. 661.
36. M. Talagrand, *Prob. Theory Related Fields* **117**, 303 (2000).
37. J. P. Bouchaud, L. Cugliandolo, J. Kurchan, M. Mézard, in *Spin Glasses and Random Fields*, A. P. Young, Ed. (World Scientific, Singapore, 1997), p. 161.
38. We thank B. Selman and J. S. Yedidia for useful exchanges. Supported in part by the European Science Foundation under the SPHINX program.

25 April 2002; accepted 19 June 2002
 Published online 27 June 2002;
 10.1126/science.1073287
 Include this information when citing this paper.

White Collar–1, a Circadian Blue Light Photoreceptor, Binding to the frequency Promoter

Allan C. Froehlich,¹ Yi Liu,^{1*} Jennifer J. Loros,^{1,2†}
 Jay C. Dunlap^{1†}

In the fungus *Neurospora crassa*, the blue light photoreceptor(s) and signaling pathway(s) have not been identified. We examined light signaling by exploiting the light sensitivity of the *Neurospora* biological clock, specifically the rapid induction by light of the clock component *frequency* (*frq*). Light induction of *frq* is transcriptionally controlled and requires two cis-acting elements (LREs) in the *frq* promoter. Both LREs are bound by a White Collar–1 (WC-1)/White Collar–2 (WC-2)–containing complex (WCC), and light causes decreased mobility of the WCC bound to the LREs. The use of in vitro–translated WC-1 and WC-2 confirmed that WC-1, with flavin adenine dinucleotide as a cofactor, is the blue light photoreceptor that mediates light input to the circadian system through direct binding (with WC-2) to the *frq* promoter.

In *Neurospora*, a wide range of processes is light sensitive, including suppression and phase shifting of circadian rhythms, phototropism of perithecial beaks (1), and carotenoid biosynthesis (initially described in the first published study of *Neurospora* in 1843) (2). The photoreceptor(s) involved in these blue light–influenced processes has not been identified, but screens in *Neurospora* for mutants involved in light perception and signaling have repeatedly turned up two indispensable loci, *wc-1* and *wc-2* (3). WC-1 and WC-2 are nuclear transcription factors con-

taining trans-activation and zinc-finger (Zn-finger) DNA binding domains (4, 5). They form a White Collar Complex (WCC) by heterodimerizing via PAS (PER ARNT SIM) domains (6, 7) and act as positive elements in light signaling, most likely through direct binding of DNA (4, 5); in true *wc-1^{KO}* and *wc-2^{KO}* strains, all examined light responses are lost (8, 9). This requirement suggested to us and others that either WC-1 or WC-2 is the photoreceptor, or that they both are required to mediate the response of an unidentified, perhaps duplicated, receptor (1, 10, 11).

In *Neurospora*, generation of circadian rhythms is dependent on WCC-mediated rhythmic production of *frq* transcript and protein, both of which are central clock components (12, 13). Light causes a rapid induction of *frq* message, the central means by which light influences the clock (14). In the absence of WC-1 or WC-2, light induction of *frq* is completely

abolished, highlighting the WCs' central role in light input to the clock (8, 9, 15).

Effects of light in vivo. To examine the contribution of transcription to the light-induced accumulation of *frq* transcript, the *frq* promoter was fused to a reporter gene, *hph*, and the resulting construct, pYL40B, was transformed into a *frq⁺* strain. Light treatment of transformants resulted in a marked increase in *hph* transcript level, similar to that of *frq* (Fig. 1A). Because only *frq* promoter sequence was fused to *hph*, light induction of the *hph* transcript, and consequently of endogenous *frq* message, is controlled at the transcriptional level.

We identified cis-acting elements mediating light induction of *frq* by transforming *frq* promoter deletion constructs into a *frq^{KO}* strain and the testing for light induction of *frq* message (Fig. 1B). Deletion of two light response elements (LREs) in the *frq* promoter decreased light induction of *frq* message. We noted an ~50% reduction with the distal LRE deleted (AF26) and an ~70% reduction with the proximal LRE deleted (AF33) (Fig. 1C). Deletion of both LREs (AF36) abolished light induction of *frq* transcript (Fig. 1C), which suggests that light induction of *frq* is controlled entirely at the transcriptional level. Both LREs were also sufficient to confer light inducibility on an *hph* reporter construct (pAF35), both individually (pAF43 and pAF44) and together (pAF45) (Fig. 1D).

The effects of the LRE deletions on circadian clock function were examined using race tubes to monitor *Neurospora*'s rhythmic conidiation (11). In a wild-type strain, transferring race tubes from light to dark results in a decrease in *frq* transcript that sets the clock to subjective dusk, after which the clock continues to run (11, 14). Control ABC1 transformants, containing the entire *frq* locus, displayed a period and phase similar to those of

Departments of ¹Genetics and ²Biochemistry, Dartmouth Medical School, Hanover, NH 03755, USA.

*Present address: Department of Physiology, University of Texas Southwestern Medical Center, Dallas, TX 75390, USA.

†To whom correspondence should be addressed. E-mail: jennifer.loros@dartmouth.edu (J.J.L.) and jay.c.dunlap@dartmouth.edu (J.C.D.)